Resonant phenomena in nonlinearly managed lattice solitons

Yaroslav V. Kartashov[1,2] and Victor A. Vysloukh[3]
[1]*ICFO–Institut de Ciencies Fotoniques, and Department of Signal Theory and Communications, Universitat Politecnica de Catalunya, 08034 Barcelona, Spain*
[2]*Physics Department, M. V. Lomonosov Moscow State University, 119899 Moscow, Russia*
[3]*Departamento de Fisica y Matematicas, Universidad de las Americas–Puebla, Santa Catarina Martir, Cholula, CP 72820, Puebla, Mexico*
(Received 6 February 2004; published 24 August 2004)

The formation of nonlinearly managed spatial solitons in Kerr-type nonlinear media with transverse periodic modulation of the refractive index is considered. The phenomenon of resonant enhancement of lattice soliton amplitude oscillations is reported. We show how the tunable discreteness and competition between such characteristic scales as the beam width and the lattice period influence propagation dynamics and properties of breathing lattice solitons.

DOI: 10.1103/PhysRevE.70.026606 PACS number(s): 42.65.Jx, 42.65.Tg, 42.65.Wi

Laser beam self-action in nonlinear waveguide lattices, including primarily the formation of discrete solitons, is very important for such practical application as all-optical soliton steering and switching (for review, see Refs. [1,2] and references therein). The diffraction properties of such systems can be controlled effectively providing rich possibilities for designing photonic devices [3,4]. The competition between transverse characteristic scales of the problem, namely the beam width and linear refractive index modulation period, gives rise to a variety of propagation scenarios [5]. Additional options are related to tunable discreteness, which alters the system properties from fully continuous to fully discrete by varying the depth of refractive index modulation [6–9].

From the other side, nonlinearity management (NLM) proved to be an effective tool in nonlinear optics. The key issue is that nonlinear structures with periodically varying nonlinearities permit the smooth tuning of the mean nonlinearity value, which, in turn, offers the possibility to control the soliton energy flow for fixed width. NLM has been successfully explored for the formation of three-dimensional light bullets [10]. It can potentially prevent beam collapse [11] and improve optical pulse transmission [12]. Fiber lasers also contain NLM-based elements [13]. Notice that the NLM concept has been recently applied to Bose-Einstein condensates using Feshbach resonance management [14–16].

In this context, photorefractive crystals are excellent candidates for experimental implementation of the lattice soliton concept [1]. Recently spatial optical solitons have been demonstrated in arrays of photoinduced waveguides [1,17,18]. Such photoinduced structures offer opportunities to vary not only the lattice period (scales competition) and refractive index modulation depth (tunable discreteness) but also the value and sign of nonlinearity (nonlinearity management) by changing the polarity of applied electric field or rotation of the polarization of light.

Here we consider the impact of NLM on propagation and excitation of lattice solitons in cubic nonlinear media with imprinted harmonic transverse modulation of the refractive index. We show that under appropriate conditions, soliton propagation in lattices (especially with big transverse periods) is accompanied with a resonant enhancement of soliton amplitude oscillations due to NLM. Tunable discreteness allows us to control not only the spatial energy distribution in lattice solitons but also their dynamical properties.

Propagation of optical radiation along the z axis of a slab waveguide with harmonic modulation of the linear refractive index in the x direction and management of cubic nonlinearity is described by the nonlinear Schrödinger equation,

$$i\frac{\partial q}{\partial \xi} = -\frac{1}{2}\frac{\partial^2 q}{\partial \eta^2} + \sigma(\xi)|q|^2 q - pR(\eta)q. \tag{1}$$

Here $q(\eta,\xi)=(L_{\mathrm{dif}}/L_{\mathrm{nl}})^{1/2}A(\eta,\xi)I_0^{-1/2}$, $A(\eta,\xi)$ is the slowly varying envelope, I_0 is the peak input intensity, $\eta=x/r_0$, r_0 is the transverse scale, $\xi=z/L_{\mathrm{dif}}$, $L_{\mathrm{dif}}=n_0\omega r_0^2/c$, $L_{\mathrm{nl}}=2c/\omega n_2 I_0$, ω is the carrying frequency, $p=L_{\mathrm{dif}}/L_{\mathrm{ref}}$ is the guiding parameter, $L_{\mathrm{ref}}=c/(\delta n\omega)$, δn is the refractive index modulation depth, function $R(\eta)=\cos(\Omega_\eta\eta)$ describes the transverse refractive index profile, Ω_η is the transverse modulation frequency, while $\sigma(\xi)=\sigma_0\{1+\mu\ \mathrm{sgn}[\cos(\Omega_\xi\xi)]\}$ describes the symmetric steplike nonlinearity map with the mean value $\sigma_0<0$ (focusing nonlinearity), longitudinal frequency Ω_ξ, and depth μ. Notice that the energy flow $U=\int_{-\infty}^{\infty}|q|^2\,d\eta$ is a conserved quantity of Eq. (1).

Scenarios of laser beam propagation in the periodic lattice can be classified using the so-called renormalized soliton approach [5]. Within the framework of this approach, the soliton shape can be approximated by $q(\eta,\xi)=q_0\,\mathrm{sech}(\chi\eta)\exp[i\phi(\eta,\xi)]$, where q_0 is the soliton amplitude, χ is the form factor or inverse width, and ϕ is the phase. Note that such a trial function does not take into account radiative losses. The evolution of the mean-square width $\langle\eta^2\rangle=U^{-1}\int_{-\infty}^{\infty}\eta^2|q|^2d\eta$ is then governed by the equation [6,7]

$$\frac{d^2}{d\xi^2}\langle\eta^2\rangle = \frac{2}{3}[\chi^2+\sigma(\xi)q_0^2] - 2p\frac{\pi\Omega_\eta/2\chi}{\sinh(\pi\Omega_\eta/2\chi)}\left[\frac{\pi\Omega_\eta/2\chi}{\tanh(\pi\Omega_\eta/2\chi)}-1\right]. \tag{2}$$

In the absence of nonlinearity management, when $\sigma(\xi)\equiv\sigma_0$,

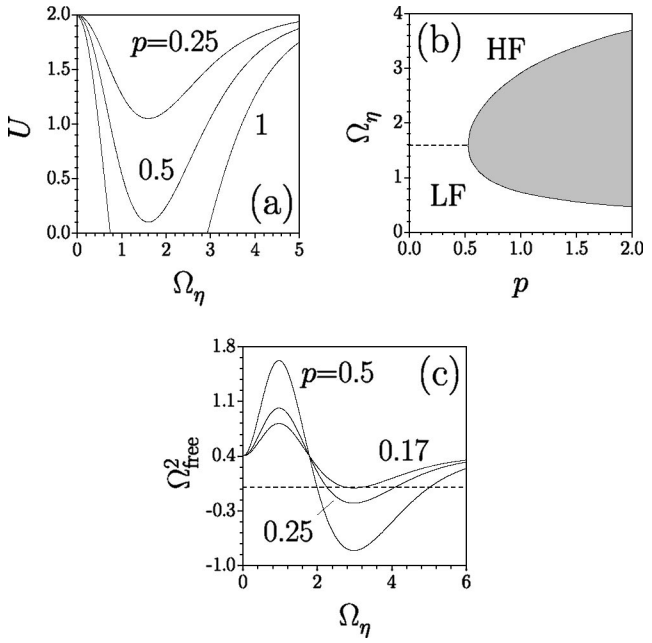

FIG. 1. Properties of renormalized solitons in the absence of NLM. (a) Energy flow vs transverse refractive index modulation frequency. (b) Cut-offs for transverse modulation frequency at (p,Ω_η) plane. (c) Squared frequency of free form-factor oscillations vs transverse modulation frequency. Horizontal dashed line in (c) stands for $\Omega_{\text{free}}^2=0$. All quantities are plotted in arbitrary dimensionless units.

Eq. (2) enables us to derive the condition of stationary lattice soliton propagation corresponding to $d\langle\eta^2\rangle/d\xi=0$ and $d^2\langle\eta^2\rangle/d\xi^2=0$. Assuming that the soliton form factor does not change upon propagation, one gets an expression for the renormalized soliton amplitude,

$$q_0^2=-\frac{\chi^2}{\sigma_0}+\frac{3p}{\sigma_0}\frac{\pi\Omega_\eta/2\chi}{\sinh(\pi\Omega_\eta/2\chi)}\left[\frac{\pi\Omega_\eta/2\chi}{\tanh(\pi\Omega_\eta/2\chi)}-1\right]. \quad (3)$$

Energy flow of the renormalized lattice soliton is given by $U=2q_0^2/\chi$. It is worth noticing that for the fixed form factor or width, the energy flow is inversely proportional to the mean value of nonlinearity σ_0, which is important from a practical point of view [19].

Properties of renormalized solitons governed by Eq. (3) in the absence of NLM are summarized in Fig. 1, where we assume $\sigma_0=-1$ and $\chi=1$ without loss of generality. Energy flow of the lattice soliton is lower than that for a soliton with the same width in a uniform medium (because of the presence of guiding structure, lower light intensity is necessary to support solitonlike propagation) only for intermediate transverse modulation frequencies Ω_η [Fig. 1(a)], while at low frequencies (when the soliton is well localized inside a single focusing channel) and at high frequencies (when the soliton covers many lattice sites), the lattice weakly affects soliton amplitude and energy flow. For weak guiding ($p\leq 0.52$, shallow lattice), the renormalized soliton exists for all values of Ω_η, but for higher modulation depths there appears a forbidden frequency gap centered around $\Omega_\eta\simeq 1.6$. The area of forbidden frequencies is shown in gray at the (p,Ω_η) plane in Fig. 1(b). This area corresponds to solitons with rather deep shape modulation (the profile of such solitons cannot be described with a sech-type function) and broadens with an increase of the guiding parameter. The forbidden gap separates the area of soliton existence into low-frequency (LF) and high-frequency (HF) domains. It is in these domains, where the linear refractive index modulation acts like a perturbation, the renormalized soliton properly describes the real soliton. Thus solitons from the LF domain are weakly affected by harmonic modulation since they are narrower than the lattice period, while the HF domain solitons smooth over several lattice sites.

In the presence of NLM, the mean-square width, amplitude, and form factor of lattice solitons breathe upon propagation. For small longitudinal modulation depths $\mu\ll 1$, it is instructive to consider the dynamics of small perturbations $\delta\chi(\xi)\ll\chi$ of the form factor χ of the stationary renormalized soliton that is related to its mean-square width as $\chi=\pi/12^{1/2}\langle\eta\rangle^{1/2}$. Taking into account only the principal harmonic of the steplike nonlinearity map and assuming $\sigma_0=-1$, $\chi=1$, one arrives at

$$\frac{d^2}{d\xi^2}\delta\chi+\left[\Omega_{\text{free}}^2-\frac{4\mu q_0^2}{\pi^2}\cos(\Omega_\xi\xi)\right]\delta\chi=\frac{4\mu q_0^2}{\pi^2}\cos(\Omega_\xi\xi), \quad (4)$$

where

$$\Omega_{\text{free}}^2=\frac{8}{\pi^2}-\frac{4q_0^2}{\pi^2}+\frac{12p}{\pi^2}\frac{\pi\Omega_\eta/2}{\sinh(\pi\Omega_\eta/2)}\left[\frac{3\pi\Omega_\eta/2}{\tanh(\pi\Omega_\eta/2)}-\frac{(\pi\Omega_\eta/2)^2[\cosh^2(\pi\Omega_\eta/2)+1]}{\tanh^2(\pi\Omega_\eta/2)}-1\right] \quad (5)$$

defines the frequency of free oscillations of the perturbed form factor along the ξ axis in the absence of NLM. As one can see from Eq. (1), resonant frequency changes periodically along the ξ axis within the band $[\Omega_{\text{free}}^2\pm 4\mu q_0^2/\pi^2]^{1/2}$. It should be pointed out that for a general-type periodic function $\sigma(\xi)=\sigma(\xi+2\pi/\Omega_\xi)$, the technique of its expansion into Fourier series can be applied as well and offers an opportunity to analyze qualitatively the dynamics of form-factor perturbation for more complicated nonlinearity maps, including nonsymmetric ones.

Figure 1(c) shows the dependence of Ω_{free}^2 on transverse modulation frequency Ω_η for different guiding parameters p. Notice that for $\Omega_\eta\to 0$ as well as for $\Omega_\eta\to\infty$, the frequency $\Omega_{\text{free}}\to 2/\pi$, which corresponds to the frequency of form-factor oscillations in the uniform medium. For $\mu\neq 0$, Eq. (4) describes forced vibrations of a parametrically driven harmonic oscillator. Therefore, in the areas with $\Omega_{\text{free}}^2>0$, the usual ($\Omega_\xi=\Omega_{\text{free}}$) and the parametric ($\Omega_\xi=m\Omega_{\text{free}}$, $m=2,3,\ldots$) resonance of soliton oscillations are possible. Physically, resonances occur because of the appropriate swinging of intrinsic soliton oscillations by the periodic increase or decrease of nonlinearity on the same or multiple frequencies. Note also that because resonance frequency is modulated along the ξ axis, there appear resonance bands rather than single resonances. In the area with $\Omega_{\text{free}}^2<0$ (lower part of the HF band), soliton response to periodical

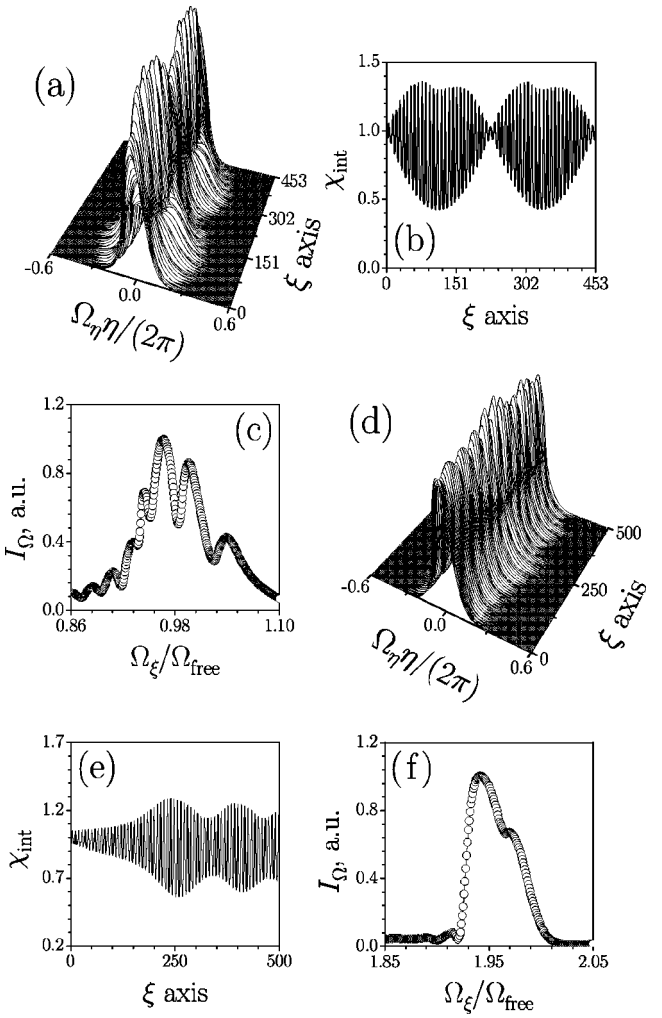

FIG. 2. Resonance enhancement of lattice soliton width oscillations in the presence of NLM. (a) Propagation dynamics of lattice soliton at $p=0.5$, $\Omega_\eta=0.5$, $\mu=0.05$, and $\Omega_\xi=0.965\Omega_{\text{free}}$ corresponding to the usual resonance. (b) Evolution of integral form factor of the soliton depicted in (a). (c) Maximal spectral intensity of the form-factor oscillations at usual resonance vs frequency ratio $\Omega_\xi/\Omega_{\text{free}}$. (d) The same as in (a) but for $\mu=0.1$ and $\Omega_\xi=1.9375\Omega_{\text{free}}$, which corresponds to the first parametric resonance. (e) Evolution of integral form factor of soliton depicted in (d). (f) Maximal spectral intensity of the form-factor oscillations at parametric resonance vs frequency ratio $\Omega_\xi/\Omega_{\text{free}}$. All quantities are plotted in arbitrary dimensionless units.

nonlinearity management is essentially nonresonant.

This simplified picture gives only a qualitative explanation of the phenomenon of resonance enhancement of soliton amplitude oscillations; real NLM soliton dynamics can be more complicated, since in some regions soliton profile may not be adequately described by a sech-type function [see the gray region in Fig. 1(b)] and NLM itself inevitably produces radiative losses (that reach up to 20% from input soliton energy for parameter ranges considered) that are not captured by the model. Nevertheless, we detected in computer simulations that key qualitative features predicted by Eq. (4) are valid.

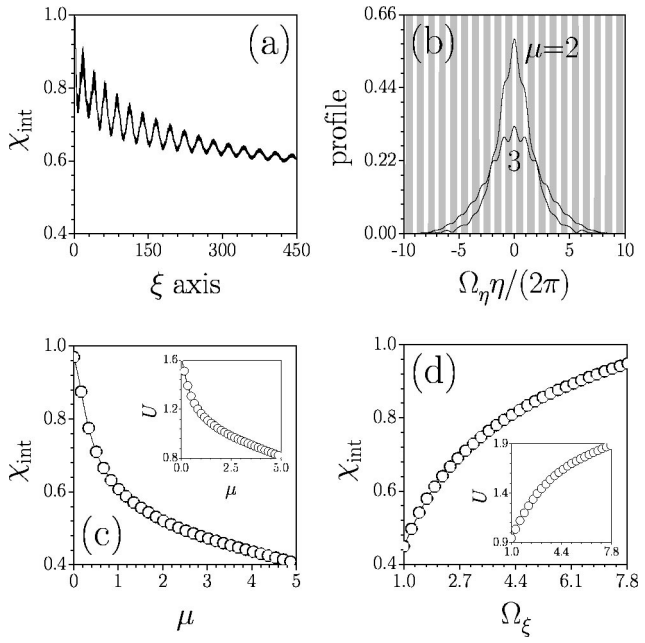

FIG. 3. Excitation of steadily breathing lattice solitons in nonresonant conditions. (a) Evolution of integral soliton form factor upon propagation at $p=0.5$, $\Omega_\eta=4$, $\Omega_\xi=4$, $\mu=1$. (b) Profiles of steadily breathing lattice solitons at $p=0.5$, $\Omega_\eta=4$, $\Omega_\xi=4$, and different depths of longitudinal modulation of refractive index. In gray regions function $R(\eta)\leq 0$, while in white regions $R(\eta)>0$. (c) Output integral form factor and energy flow (inset) vs depths of longitudinal modulation at $p=0.5$, $\Omega_\eta=4$, $\Omega_\xi=4$. (d) Output integral form factor and energy flow (inset) vs longitudinal modulation frequency at $p=0.5$, $\Omega_\eta=4$, $\mu=0.5$. All quantities are plotted in arbitrary dimensionless units.

To show this, we solved Eq. (1) numerically using the renormalized soliton [Eq. (3)] as an input. Upon numerical integration, we followed the dynamics of the integral form factor $\chi_{\text{int}}(\xi)=3U^{-2}\int_{-\infty}^{\infty}|q|^4 d\eta$ that coincides with χ for the sech-type soliton, and correctly characterizes the behavior of the central energy-carrying part of the beam even in the presence of radiation, discriminating the low-intensity background.

Figure 2(a) shows propagation of the soliton belonging to the LF domain under conditions of usual resonance $\Omega_\xi \approx \Omega_{\text{free}}$, while the corresponding dependence of the integral form factor on propagation distance is depicted in Fig. 2(b). The strong linear growth of oscillations amplitude is evident at the initial stage of propagation ($\xi<50$), while at longer distances one has a beating process with periodic restoration of input profile. This behavior is typical for dumped nonlinear oscillators. It is the nonlinearity of large-amplitude form-factor oscillations [not taken into account in Eq. (4)] that results in frequency detuning and periodic diminishing of amplitude. Fourier transform $\delta\chi(\Omega)$ of the dependence $\delta\chi(\xi)$ has a global maximum in the vicinity of Ω_ξ. The resonance curve, defined here as the dependence of the peak spectral intensity of form-factor oscillations $I_\Omega=\max|\delta\chi(\Omega)|^2$ on NLM frequency Ω_ξ, is shown in Fig. 2(c). It should be pointed out that the resonance is strong (almost two orders of magnitude in intensity), relatively narrow (approximately

10% of the relative frequency detuning), and that the resonant curve is deeply modulated. The source of this modulation is quite clear: the frequency of free oscillations Ω_{free} is altered periodically on ξ within the interval of the width $\delta\Omega_{\text{free}} \simeq 4\mu q_0^2/\pi^2\Omega_{\text{free}}$ [Eq. (4)], i.e., this width determines the modulation period $T_{\text{mod}} \approx 2\pi/\delta\Omega_{\text{free}}$ of the resonance curve. Notice that the renormalized soliton from the LF band is well localized within one focusing channel. During the soliton spreading, neighboring defocusing channels are gradually involved, the effective focusing action saturates, and the resonant frequency diminishes, which corresponds to soft-type nonlinearity. That is, this nonlinearity leads to asymmetry of the resonance curve [Fig. 2(c)].

Figures 2(d)–2(f) illustrate lattice soliton behavior under conditions of first-order parametric resonance ($\Omega_\xi \approx 2\Omega_{\text{free}}$). This resonance is also quite strong, and the corresponding resonance curve is even narrower than that for usual resonance. Notice that higher-order parametric resonances are also possible.

Out of the resonance bands, steadily breathing lattice solitons are formed. In some cases, their profiles can be found with the numerical averaging method (see, e.g., [20] and references therein). Here we obtain such solitons by the direct launching of renormalized solitons into NLM structure and their subsequent propagation at considerable distances ξ. Thus, Fig. 3(a) shows the evolution of the integral form factor for the soliton from the HF band launched into NLM structure with considerable longitudinal modulation depth $\mu=1$. Soliton dynamics is nonresonant and the core lattice soliton is formed at $\xi \to \infty$. Formation of the true breathing lattice soliton from the renormalized hyperbolic secant profile starts with spectral broadening and the appearance of sidebands on spatial frequencies $\pm\Omega_\eta$ due to the phase modulation produced by the harmonic lattice. Sidebands are parametrically amplified because of the cubic nonlinearity, and when parametric amplification saturates steadily, the breathing soliton is formed. Profiles of lattice solitons are depicted in Fig. 3(b) for different values of longitudinal modulation depth. The growth of μ leads to the delocalization of the beam and diminishes its energy flow. Figures 3(c) and 3(d) illustrate the dependences of the output integral form factor and energy flow on longitudinal modulation depth and frequency, respectively. The output energy flow and the integral form factor decrease monotonically with growth of μ, while an increase of modulation frequency results in an increase of these soliton parameters.

In conclusion, we have found the parameter areas where soliton propagation in NLM structures is accompanied by resonant growth of the amplitude oscillations, and the areas where soliton response on periodic nonlinearity management is essentially nonresonant, so that steadily breathing solitons can be formed. NLM significantly enriches the possibilities of light beam control since the spatial soliton energy is defined mainly by the average nonlinearity, and its localization depends on the nonlinearity modulation depth and frequency.

Financial support from CONACyT under Grant No. U39681-F is gratefully acknowledged by V.A.V. Y.V.K. acknowledges support by the Generalitat de Catalunya.

[1] J. W. Fleischer *et al.*, Nature (London) **422**, 147 (2003).
[2] D. N. Christodoulides, F. Lederer, and Y. Silberberg, Nature (London) **424**, 817 (2003).
[3] H. S. Eisenberg *et al.*, Phys. Rev. Lett. **85**, 1863 (2000).
[4] T. Pertsch *et al.*, Phys. Rev. Lett. **88**, 093901 (2002).
[5] R. Scharf and A. R. Bishop, Phys. Rev. E **47**, 1375 (1993).
[6] Y. V. Kartashov *et al.*, Opt. Lett. **29**, 766 (2004).
[7] Y. V. Kartashov *et al.*, Opt. Lett. **29**, 1102 (2004).
[8] Y. V. Kartashov *et al.*, Opt. Express **12**, 2831 (2004).
[9] Y. V. Kartashov, A. A. Egorov, L. Torner, and D. N. Christodoulides (unpublished).
[10] L. Torner *et al.*, Opt. Commun. **199**, 277 (2001).
[11] I. Towers and B. A. Malomed, J. Opt. Soc. Am. B **19**, 537 (2002).
[12] M. J. Ablowitz and T. Hirooka, J. Opt. Soc. Am. B **19**, 425 (2002).
[13] F. O. Iiday and F. W. Wise, J. Opt. Soc. Am. B **19**, 470 (2002).
[14] F. K. Abdullaev *et al.*, Phys. Rev. A **68**, 053606 (2003).
[15] P. G. Kevrekidis *et al.*, Phys. Rev. Lett. **90**, 230401 (2003).
[16] D. E. Pelinovsky, P. G. Kevrekidis, and D. J. Frantzeskakis, Phys. Rev. Lett. **91**, 240201 (2003).
[17] N. K. Efremidis *et al.*, Phys. Rev. E **66**, 046602 (2002).
[18] D. Neshev *et al.*, Opt. Lett. **28**, 710 (2003).
[19] S. Turitsyn, T. Schaefer, and V. Mezentsev, Phys. Rev. E **58**, R5264 (1998).
[20] Y. V. Kartashov *et al.*, Phys. Rev. E **68**, 026613 (2003).